A proposal of finite-element analysis considering two-dimensional magnetic properties

Koji Fujiwara
Okayama University

Takayuki Adachi
Okayama University

Norio Takahashi
Okayama University

A Proposal of Finite-Element Analysis Considering Two-Dimensional Magnetic Properties

Koji Fujiwara, Takayuki Adachi, and Norio Takahashi, *Fellow, IEEE*

***Abstract*—A technique for analyzing the magnetic field in anisotropic material using the effective anisotropic reluctivity proposed by Enokizono is examined. It is shown that the Enokizono model can be transformed into another model having a conventional form. By expanding the examination of such a conventional form, a new finite element formulation for taking account of the two-dimensional (2-D) magnetic property is proposed. As the modeling of the 2-D magnetic property at the high flux density region is important in the practical analysis of the magnetic device, the extrapolation method of the magnetic property is examined. It is shown that the Bézier interpolation is fairly effective to stabilize the convergence characteristic of the Newton–Raphson (N–R) iteration in the nonlinear magnetic field analysis, taking account of the 2-D magnetic property.**

***Index Terms*—2-D magnetic properties, anisotropy, Bézier interpolation, finite-element method.**

I. Introduction

THERE are many papers examining how to take account of two-dimensional (2-D) magnetic properties of grain-oriented silicon steel [1], [2]. Especially, Enokizono proposed various techniques to model the 2-D properties, such as a method using the effective anisotropic reluctivity [1]. The nonlinear magnetic field analysis of such anisotropic material is not easy, because the Newton–Raphson (N–R) iteration sometimes does not converge [3]. The fact that the 2-D properties used in the calculation almost always include measurement error is also the reason for the difficulty of the convergence of the N–R iteration.

In this paper, the method using the effective anisotropic reluctivity is examined in detail, and an efficient modeling technique of 2-D properties is examined in order to realize the precise and fast analysis of magnetic fields. In this technique, the anisotropic reluctivity is treated as a function of the amplitudes of $\boldsymbol{B}$ (flux density), $\boldsymbol{H}$ (magnetic field strength), θ_B (direction of $\boldsymbol{B}$), and θ_H (direction of $\boldsymbol{H}$). The finite-element formulation for such a technique is shown. Moreover, in order to obtain a stable convergence of the N–R iteration, a method of extrapolating the 2-D magnetic property at the high flux density region is proposed. The Bézier interpolation technique is applied for smoothing the measured data. It is shown using a simple magnetic circuit composed of grain-oriented silicon steel that such extrapolation and smoothing techniques are considerably effective for the fast convergence of the N–R iteration.

Manuscript received July 5, 2001; revised October 25, 2001.

The authors are with the Department of Electrical and Electronic Engineering, Okayama University, Okayama 700-8530, Japan (e-mail: fujiwara@eplab.elec.okayama-u.ac.jp; adachi@eplab.elec.okayama-u.ac.jp; norio@eplab.elec.okayama-u.ac.jp).

Publisher Item Identifier S 0018-9464(02)02531-1.

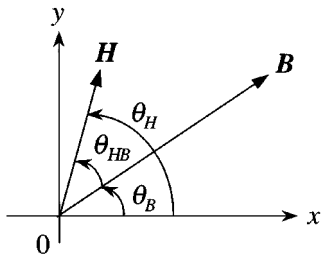

Fig. 1. $\boldsymbol{B}$ and $\boldsymbol{H}$ vectors in anisotropic material.

II. New Expression

A. Reluctivity of Anisotropic Material

In anisotropic material, the direction of $\boldsymbol{H}$ vector is different from that of $\boldsymbol{B}$ vector, as shown in Fig. 1. θ_{HB} is the angle between $\boldsymbol{H}$ and $\boldsymbol{B}$ vectors shown in Fig. 1. The effective anisotropic reluctivity [1] is defined by

$$\nu_{\text{eff}} = \frac{|\boldsymbol{H}|}{|\boldsymbol{B}|}. \tag{1}$$

By some algebra, the reluctivity ν is finally given by

$$\nu = \begin{bmatrix} \nu_{xx} & \nu_{xy} \\ \nu_{yx} & \nu_{yy} \end{bmatrix} = \begin{bmatrix} \nu_{\text{eff}}\cos\theta_{HB} & -\nu_{\text{eff}}\sin\theta_{HB} \\ \nu_{\text{eff}}\sin\theta_{HB} & \nu_{\text{eff}}\cos\theta_{HB} \end{bmatrix} = \begin{bmatrix} \nu_{xx} & \nu_{xy} \\ -\nu_{xy} & \nu_{xx} \end{bmatrix}. \tag{2}$$

This is the reluctivity of Enokizono type. Equation (2) can be rewritten as

$$\nu = \begin{bmatrix} \nu_{\text{eff}}\cos\theta_{HB} - \nu_{\text{eff}}\dfrac{B_y}{B_x}\sin\theta_{HB} & 0 \\ 0 & \nu_{\text{eff}}\dfrac{B_x}{B_y}\sin\theta_{HB} + \nu_{\text{eff}}\cos\theta_{HB} \end{bmatrix}. \tag{3}$$

By using the relationships of $H_x = H\cos\theta_H$, $H_y = H\sin\theta_H$, and $\theta_{HB} = \theta_H - \theta_B$, and after some algebra, the following expression of reluctivity can be obtained:

$$\nu = \begin{bmatrix} \dfrac{H\cos\theta_H}{B\cos\theta_B} & 0 \\ 0 & \dfrac{H\sin\theta_H}{B\sin\theta_B} \end{bmatrix} = \begin{bmatrix} \nu_x & 0 \\ 0 & \nu_y \end{bmatrix}. \tag{4}$$

Equation (4) denotes that the reluctivity is represented as a function of B, θ_B, H, and θ_H, whereas the reluctivity of Enokizono type in (3) is represented as a function of B, θ_B, ν_{eff}, and θ_{HB}. Although the style of representation of reluctivity is almost the same for (3) and (4), the convergence of the N–R iteration may be different. Then, the effectiveness of the representation of (4) is examined.

B. Finite-Element Formulation

The derivative $\partial G_i^{(e)}/\partial A_j$ of the weighted residual by the vector potential A_j is given by

$$\frac{\partial G_i^{(e)}}{\partial A_j} = \frac{1}{4\Delta}\left(\nu_x d_i d_j + \nu_y c_i c_j\right) + \frac{\partial \nu_x}{\partial A_j}\frac{1}{4\Delta}\sum_{k=1}^{3} d_i d_{ke} A_{ke} + \frac{\partial \nu_y}{\partial A_j}\frac{1}{4\Delta}\sum_{k=1}^{3} c_i c_{ke} A_{ke} \quad (5)$$

where c_i, d_i are the functions of coordinates of nodes, and Δ is the area of the first-order triangular finite element e.

$\partial \nu_x/\partial A_j$ and $\partial \nu_y/\partial A_j$ are given by (6) and (7), shown at the bottom of the page. $\partial H/\partial B$, $\partial H/\partial \theta_B$, $\partial \theta_H/\partial B$, and $\partial \theta_H/\partial \theta_B$ can be calculated using the magnetization property of grain-oriented silicon steel shown in Fig. 2, which are measured using the completely closed magnetic path type of single sheet tester with double excitation [4]. The grade of the silicon steel is JIS: 35G165 (thickness: 0.35 mm, $W_{17/50} \leq 1.65$ W/kg).

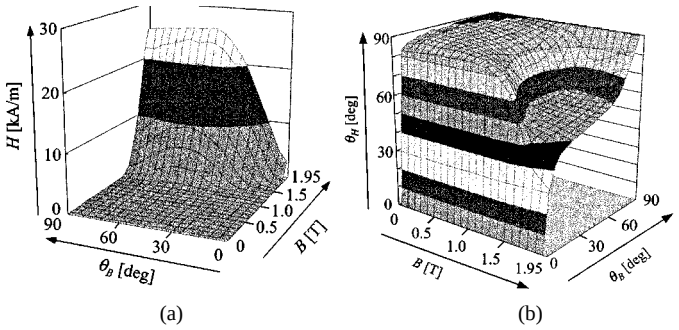

Fig. 2. 2-D magnetization property measured. (a) $H-(B,\ \theta_B)$ function. (b) $\theta_H-(B,\ \theta_B)$ function.

$$\frac{\partial \nu_x}{\partial A_j} = \frac{1}{B\cos\theta_B}\left[\cos\theta_H\left(\frac{\partial H}{\partial B}\right) - H\sin\theta_H\left(\frac{\partial \theta_H}{\partial B}\right) + \left(\frac{\left\{\left(\frac{\partial H}{\partial B}\right)\cos\theta_H - H\sin\theta_H\left(\frac{\partial \theta_H}{\partial B}\right)\right\}B - H\cos\theta_H}{B}\right)\right]\frac{\partial B}{\partial A_j} + \frac{1}{B\cos\theta_B}\left[\cos\theta_H\left(\frac{\partial H}{\partial \theta_B}\right) - H\sin\theta_H\left(\frac{\partial \theta_H}{\partial \theta_B}\right) + \left(\frac{\left\{\left(\frac{\partial H}{\partial \theta_B}\right)\cos\theta_H - H\sin\theta_H\left(\frac{\partial \theta_H}{\partial \theta_B}\right)\right\}\cos\theta_B + H\cos\theta_H\sin\theta_B}{\cos\theta_B}\right)\right]\frac{\partial \theta_B}{\partial A_j} \quad (6)$$

$$\frac{\partial \nu_y}{\partial A_j} = \frac{1}{B\sin\theta_B}\left[\sin\theta_H\left(\frac{\partial H}{\partial B}\right) + H\cos\theta_H\left(\frac{\partial \theta_H}{\partial B}\right) + \left(\frac{\left\{\left(\frac{\partial H}{\partial B}\right)\sin\theta_H + H\cos\theta_H\left(\frac{\partial \theta_H}{\partial B}\right)\right\}B - H\sin\theta_H}{B}\right)\right]\frac{\partial B}{\partial A_j} + \frac{1}{B\sin\theta_B}\left[\sin\theta_H\left(\frac{\partial H}{\partial \theta_B}\right) + H\cos\theta_H\left(\frac{\partial \theta_H}{\partial \theta_B}\right) + \left(\frac{\left\{\left(\frac{\partial H}{\partial \theta_B}\right)\sin\theta_H + H\cos\theta_H\left(\frac{\partial \theta_H}{\partial \theta_B}\right)\right\}\sin\theta_B - H\sin\theta_H\cos\theta_B}{\sin\theta_B}\right)\right]\frac{\partial \theta_B}{\partial A_j} \quad (7)$$

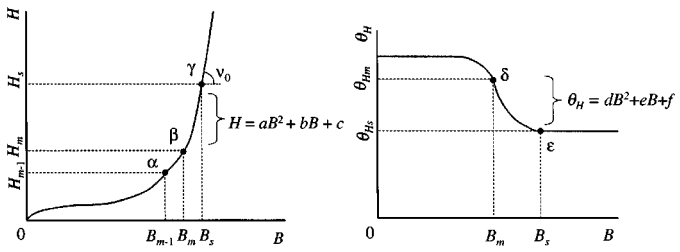

(a) (b)

Fig. 3. Techniques of extrapolation at high flux density. , θ_{Hm}, B_m: maximum values measured. H_s, θ_{Hs}, B_s: values at saturation point. (a) $H - B$. (b) $\theta_H - B$.

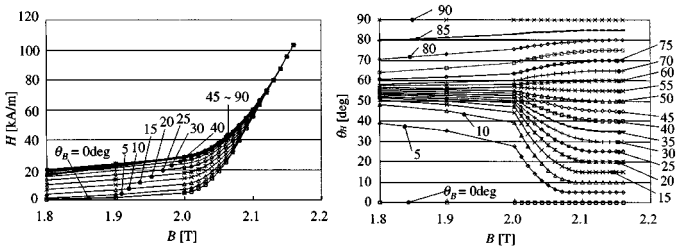

(a) (b)

Fig. 4. Curves extrapolated at various θ_Bs at high flux density region. (a) $H - B$. (b) $\theta_H - B$.

III. Methods of Modeling

A. Extrapolation at High Flux Density Region

In order to obtain a stable convergence, it is necessary to represent precisely the magnetization property up to saturation. However, it is considerably difficult to carry out the measurement at very high flux density region over 2 T. Therefore, a technique of extrapolation was proposed. After saturation, the gradient of B–H curve is equal to the permeability of vacuum ($\mu_0 = 1/\nu_0$), and the direction of $\boldsymbol{H}$ is equal to that of $\boldsymbol{B}$ ($\theta_H = \theta_B$). Fig. 3(a) shows the extrapolation of H–B function. H over the measurement limit is approximated by a quadratic function of B as follows:

$$H = aB^2 + bB + c \tag{8}$$

where a, b, and c are coefficients. The value at β and the gradient ν_0 at point γ are given, and the gradient at point β is calculated as $(H_m - H_{m-1})/(B_m - B_{m-1})$. Then, unknown variables B_s (saturation flux density), a, b, and c are determined. Fig. 3(b) shows the extrapolation of θ_H–B function. θ_H is defined as a quadratic function of B as follows:

$$\theta_H = dB^2 + eB + f \tag{9}$$

where d, e, and f are coefficients. The values at points δ and ε and the gradient (= zero) at point ε are given. Then, the coefficients, d, e, and f are obtained. Fig. 4 shows the H–B and θ_H–B curves extrapolated at various θ_Bs.

B. Bézier Interpolation

When the N–R method is applied to the nonlinear analysis, the calculation of the derivatives, $\partial H/\partial B$, $\partial H/\partial \theta_B$, $\partial \theta_H/\partial B$, and $\partial \theta_H/\partial \theta_B$, is required. In order to get a stable convergence for nonlinear iteration, the smooth approximation of measured

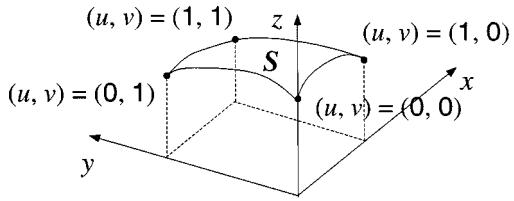

Fig. 5. Bézier interpolation.

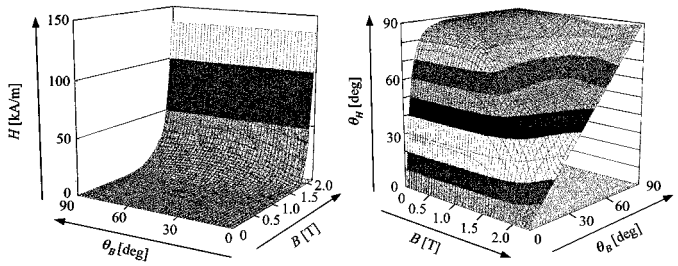

(a) (b)

Fig. 6. Bézier surfaces of 2-D magnetization property. (a) $H - (B, \theta_B)$. (b) $\theta_H - (B, \theta_B)$.

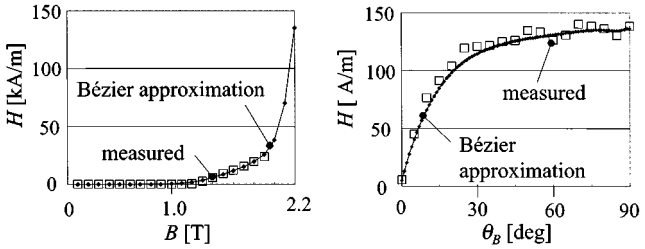

(a) (b)

Fig. 7. Comparison between measured curve and Bézier interpolation. (a) $H - B\,(\theta_B = 45°)$. (b) $H - \theta_B\,(B = 0.5\mathrm{T})$.

2-D magnetic properties shown in Fig. 2 is necessary. Then, 3-D functions, H–(B, θ_B) and θ_H–(B, θ_B), are smoothly interpolated by using the Bézier approximation shown in Fig. 5. In this case, x and y correspond to B and θ_B, respectively. z corresponds to H or θ_H. Then, the approximated values S_x, S_y, and S_z in the x, y, and z components are given by

$$\boldsymbol{S} = \sum_{i=0}^{n}\sum_{j=0}^{m} \boldsymbol{k}_{ij} B_i^n(u) B_j^m(v)$$

$$\boldsymbol{S} = [S_x \quad S_y \quad S_z]^{\mathrm{T}} \qquad \boldsymbol{k}_{ij} = [x_{ij} \quad y_{ij} \quad z_{ij}]^{\mathrm{T}}$$

$$B_i^n(u) = {}_nC_i u^i (1-u)^{n-i} \qquad B_j^m(v) = {}_mC_j v^j (1-v)^{m-j}$$

$${}_nC_i = \frac{n!}{i!(n-i)!} \tag{10}$$

where m and n denote the numbers of measured points in u and v directions. For example, x_{ij} is the measured value of B at $u = i$ and $v = j$. The maximum values of them are normalized to unity, and the minimum values are set to zero. In order to utilize the Bézier interpolation, first, the values of H (or θ_H) are sampled or interpolated at lattice points of B and θ_B, then the Bézier interpolation is carried out. Fig. 6 shows the magnetization property approximated by the Bézier interpolation. Fig. 7 shows the comparison between the measured curve and Bézier

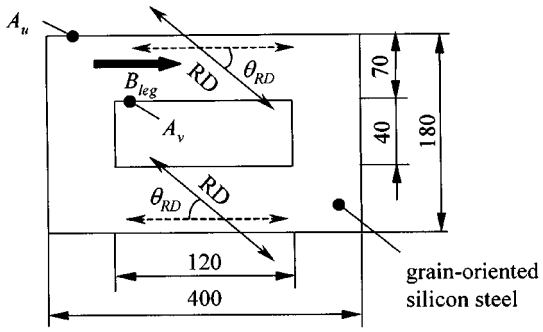

Fig. 8. Analyzed model.

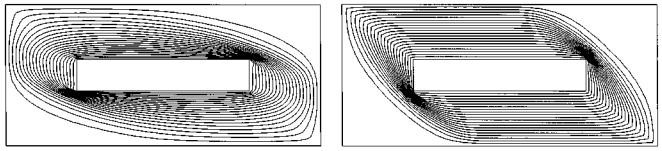

(a) (b)

Fig. 9. Flux distributions ($B_{\rm leg} = 0.3$ T). (a) $\theta_{RD} = 15°$. (b) $\theta_{RD} = 45°$.

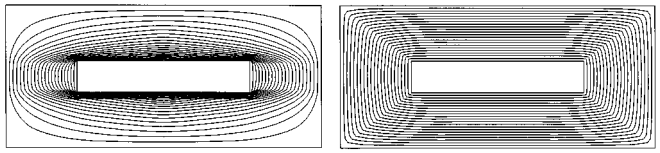

(a) (b)

Fig. 10. Flux distribution ($\theta_{RD} = 0°$). (a) $B_{\rm leg} = 0.1$T. (b) $B_{\rm leg} = 1.7$T.

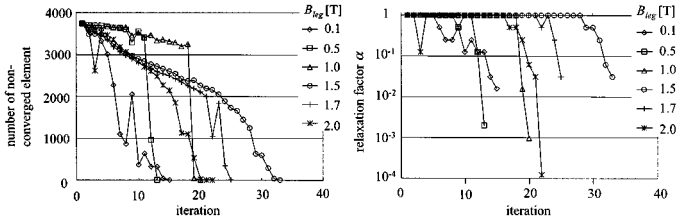

(a) (b)

Fig. 11. Convergence characteristics ($\theta_{RD} = 0°$).

interpolation. The figure denotes the effectiveness of the Bézier interpolation.

IV. Verification

A grain-oriented silicon steel having a rectangular hole, shown in Fig. 8, is used for verification. The Dirichlet boundary condition (Au, Av) is given on the inner and outer sides. $(Au - Av)/0.07$ is equal to the average flux density $B_{\rm leg}$. In order to get a converged result, the relaxation factor α [5] is used. The convergence characteristic is examined by changing the applied flux density, $B_{\rm leg}$, and the angle, θ_{RD}, of the rolling direction.

Fig. 9 shows examples of flux distribution. When the measured raw data is used, the iteration is not converged, as shown in Table I. The behavior of the number of nonconverged elements and the relaxation factor α is examined by changing the flux density $B_{\rm leg}$. Fig. 10 shows the flux distributions at $B_{\rm leg} =$ 0.1 T and 1.7 T. A typical flux distributions under the 2-D magnetization property [3] at different flux density can be obtained, and these results are reasonable. Fig. 11 shows the convergence behavior. α is equal to unity during early several iterations, and then reduces quickly when the nonlinear analysis is converged. The converged result could not obtained when the relaxation factor α was not utilized. It has been understood that the representation of the 2-D magnetization property using the extrapolation and Bézier interpolation and the introduction of the relaxation factor α is strongly effective.

TABLE I
NUMBER OF NONLINEAR ITERATIONS

(a) θ_{RD} = 45deg

extrapolation and Beziér interpolation	B_{leg} [T]				
	0.1	0.3	0.5	0.7	1.0
without (raw data)	-	-	-	-	-
with	19	25	41	43	91

(b) B_{leg} = 0.5T

extrapolation and Beziér interpolation	θ_{RD} [deg]				
	15	30	45	60	75
without (raw data)	-	-	-	-	-
with	138	41	41	38	30

Note: The "-"mark means that nonlinear iteration cannot be converged.

V. Conclusion

The obtained results can be summarized as follows.

1) A new finite-element formulation for taking account of the 2-D magnetization property has been proposed.
2) In order to analyze at high flux density region, how to extrapolate H over the measurement limit is shown.
3) Differential coefficients, such as $\partial H/\partial B$, $\partial H/\partial\theta_B$, $\partial\theta_H/\partial B$, and $\partial\theta_H/\partial\theta_B$, which are necessary in the Newton–Raphson iteration, can be effectively obtained by using the Bézier interpolation technique. It is shown that the Bézier interpolation is strongly necessary to get a converged result taking account of the 2-D magnetization property.

References

[1] M. Enokizono and N. Soda, "Finite-element analysis of transformer model core with measured reluctivity," *IEEE Trans. Magn.*, vol. 33, pp. 4110–4112, May 1997.
[2] T. Péra, F. Ossart, and T. Waeckerle, "Field computation in nonlinear anisotropic sheets using the coenergy model," *IEEE Trans. Magn.*, vol. 29, pp. 2425–2427, June 1993.
[3] T. Nakata, K. Fujiwara, N. Takahashi, M. Nakano, and N. Okamoto, "An improved numerical analysis of flux distributions in anisotropic materials," *IEEE Trans. Magn.*, vol. 30, pp. 3395–3398, May 1994.
[4] M. Nakano, H. Nishimoto, K. Fujiwara, and N. Takahashi, "Improvements of single sheet testers for measurement of 2-D magnetic properties up to high flux density," *IEEE Trans. Magn.*, vol. 35, pp. 3965–3967, May 1999.
[5] K. Fujiwara, T. Nakata, N. Okamoto, and K. Muramatsu, "Method for determining relaxation factor for modified Newton–Raphson method," *IEEE Trans. Magn.*, vol. 29, pp. 1962–1965, Feb. 1993.